

J. Phys. A: Math. Gen.

Bethe Ansatz solution of a decagonal rectangle triangle random tiling.

Jan de Gier and Bernard Nienhuis

Instituut voor Theoretische Fysica, Universiteit van Amsterdam, Valckenierstraat 65,
1018 XE Amsterdam, The Netherlands. †

Abstract. A random tiling of rectangles and triangles displaying a decagonal phase is solved by Bethe Ansatz. Analogously to the solutions of the dodecagonal square triangle and the octagonal rectangle triangle tiling an exact expression for the maximum of the entropy is found.

PACS numbers: 05.20.-y, 05.50.+q, 04.20.Jb, 61.44.Br

Short title: Solution of a decagonal random tiling

April 12, 2018

† Electronic mail addresses: degier@phys.uva.nl and nienhuis@phys.uva.nl
FAX: +(31) 20 525 5778

1. Introduction

The discussion on the stability of quasi-crystals has not resulted in a general consensus yet. Even very recently, arguments against [1] and in favour of [2] the random tiling scenario have appeared in the literature. It has also been suggested that the entropically stabilised state results from quasi-crystal growth [3]. From the point of view of statistical mechanics random tiling models are very interesting, not in the least because some of them allow for an exact solution. This means that one is able to derive exact expressions for the entropy and other thermodynamic quantities. In this paper we present a random tiling with a decagonal phase which is solvable by the Bethe Ansatz method, very much in analogy with the dodecagonal square-triangle and the octagonal rectangle-triangle tilings [4, 5, 6, 7]. The random tiling with a decagonal phase is the ensemble of tilings of the plane by rectangles and isosceles triangles with sides of length 1 and $l = 2\sin(\pi/5) = \sqrt{2+\tau}/\tau$, where $\tau = (\sqrt{5} + 1)/2$ is the golden mean. Cockayne [8] devised an inflation rule for this set of tiles that constructs a tiling with decagonal symmetry. This tiling corresponds to a maximally dense decagonal disc packing under the condition that nearest neighbour vectors are limited to certain directions. The *random* tiling with additional constraints has been studied by Oxborrow and Mihalkovič [9] to model d-AlPdMn. More recently, Roth and Henley [10] used the rectangle-triangle random tiling and some of its sub-ensembles to model decagonal quasi-crystal structures resulting from a molecular dynamics simulation.

One of the main goals in statistical mechanics is the calculation of the partition sum which, for random tilings, is the weighted sum over all possible tiling configurations. To be able to enumerate all possible tilings we use the transfer matrix method, for which it is convenient to transform the tiling to a model on the square lattice. This transformation is depicted in figure 1. The triangles always come in pairs which are denoted by t_1, \dots, t_5 corresponding to their five different orientations. Similarly the five different orientations of the rectangles are labeled by r_i . The decorations on the deformed tiles are such that continuity of the decorating lines is equivalent to the restriction that the tiles fit together without gaps or overlaps. In this way every decorated tiling of the lattice with the deformed tiles corresponds to an allowed tiling of the plane by the original rectangles and triangles. Using this transformation every vertex of the tiling falls on a vertex of the square lattice, though the reverse is not true. The partition sum of the deformed model on the lattice is now defined by

$$Z = \sum_{\mathcal{C}} \prod_{i=1}^5 r_i^{N_{r_i}(\mathcal{C})} t_i^{N_{t_i}(\mathcal{C})}, \quad (1)$$

where the sum is over all possible configurations \mathcal{C} . For a given configuration \mathcal{C} , we denote the number of deformed rectangles r_i by $N_{r_i}(\mathcal{C})$ and the number of deformed triangles t_i by $N_{t_i}(\mathcal{C})$. The partition sum is thus a weighted sum where each deformed

triangle t_i and each deformed rectangle r_i is assigned a weight t_i and r_i respectively. The partition sum (1) is equal the partition sum for the tiling, provided that one chooses the weights of the deformed tiles properly [11]. The latter is a consequence of the transformation which changes the areas of the various tiles differently.

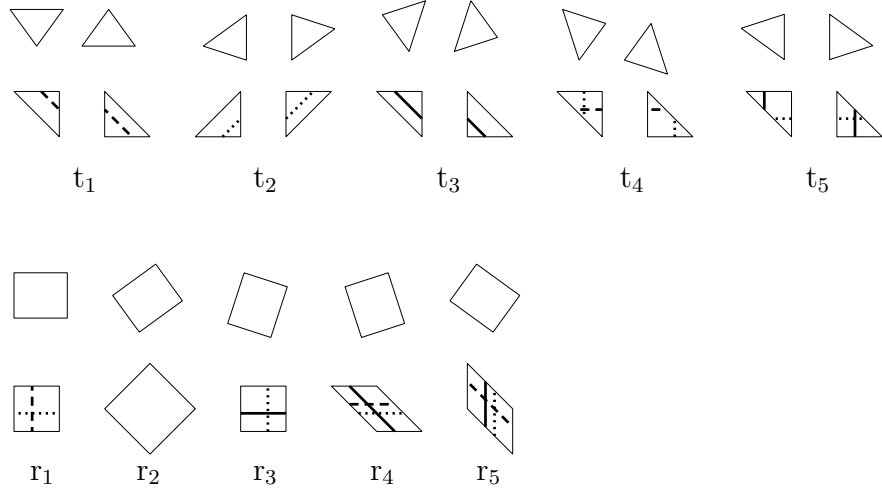


Figure 1. Tiles of the the tenfold tiling with rectangles and triangles and their deformations to the regular square lattice. The five different orientations of the pairs of triangles and those of the rectangles are denoted by t_i and r_i respectively.

The definition of the transfer matrix \mathbf{T} of the deformed model is the obvious one on the square lattice. The horizontal edges of the square lattice can be in one out of five possible states, represented by the presence or absence of the decorating lines. The transfer matrix elements T_{ij} between two sequences i and j of such horizontal edges is equal to the product of the weights of the deformed tiles that fit in between i and j . As is well known, the partition sum per row in the thermodynamic limit is given by the largest eigenvalue of the transfer matrix. The free energy is then given by the logarithm of this largest eigenvalue.

Recall that according to the random tiling hypotheses the entropy per area may be written as [12]

$$\sigma_a = \sigma_{a,0} - \frac{1}{4}K_1I_1 - \frac{1}{4}K_2I_2 - \frac{1}{2}K_3I_3, \quad (2)$$

where the I_j are the quadratic phason strain invariants for the 3×2 phason strain tensor. The goal of our work is to calculate the residual entropy $\sigma_{a,0}$ and the phason strain elastic constants K_j . In section 3 we derive the Bethe Ansatz (BA) equations that diagonalise the transfer matrix for this model and which already give a huge reduction of the numerical problem. It turns out that for this tiling the method of Kalugin [5, 7] is applicable to solve these BA equations. This then enables us to calculate the residual entropy for this tiling exactly. The calculation of the elastic constants poses some

problems and in this paper we will concentrate on the maximum only. It will be shown that the maximum of the entropy per vertex of this decagonal random tiling model is given by

$$\sigma_v = \frac{1}{2} \left(\log \frac{5^5}{4^4} - 2\sqrt{5} \log \tau \right). \quad (3)$$

2. Degrees of freedom

In principle there are fifteen partial densities for this tiling, corresponding to the ten different orientations of the triangles and the five different orientations of the rectangles. Since the triangles always occur in pairs, we are left with ten degrees of freedom. One of these is removed by the fact that the total area is constant. Furthermore, there are three nonlinear geometrical constraints, so that the phase space of this random tiling is six-dimensional. The geometrical constraints are derived in the following.[†] The first thing to note is that the triangles can be viewed as domain walls between patches consisting solely of one type of rectangle. This phenomenon is similar to what happens in dodecagonal square-triangle and the octagonal rectangle-triangle tilings. In our choice of decoration in figure 1 it is easily seen that between patches consisting only of the tile r_2 there are three different types of domain wall, denoted by the solid, dotted and dashed lines. Two types of domain wall run from bottom right to top left. They are drawn as solid and dashed lines and we denote their number by n_1 and n_2 respectively. The other type of domain wall runs from bottom left to top right and is drawn as a dotted line. Their number is given by m . We denote the average number of triangles and rectangles per layer by n_{t_i} and n_{r_i} respectively. It is then easily seen from figure 1 that

$$\begin{aligned} n_1 &= \frac{1}{2}(n_{t_3} + n_{t_5}) + n_{r_4} + n_{r_5}, \\ n_2 &= \frac{1}{2}n_{t_1} + n_{r_1} + n_{r_5}, \\ m &= \frac{1}{2}(n_{t_2} + n_{t_4}) + n_{r_3} + n_{r_5}. \end{aligned} \quad (4)$$

Let p_1 be the number of layers such that each dotted line crosses each dashed line once. The number of such crossings in this patch of size $p_1 N$ is then

$$n_2 m = p_1 (n_{r_1} + n_{r_5} + \frac{1}{2} n_{t_4}). \quad (5)$$

Similarly, if p_2 is the number of layers such that each dotted line crosses each solid line once, and q the number of layers such that each dashed line crosses each solid line once

[†] This argument makes use of the periodic boundary conditions imposed by placing the lattice model on a cylinder. We believe that for free boundary conditions modified versions of such constraints hold, involving the configuration of the boundary.

we find

$$\begin{aligned} n_1 m &= p_2(n_{r_3} + n_{r_4} + \frac{1}{2}n_{t_5}), \\ n_1 n_2 &= q(n_{r_4} + n_{r_5}). \end{aligned} \quad (6)$$

The numbers p_1 , p_2 and q can also be calculated in another way. For this, it is convenient to introduce the average shift per layer (s_1 , s_2 and s_m) of each domain wall. These are given by

$$\begin{aligned} s_1 &= -1 + \frac{1}{n_1}(n_{r_5} - n_{r_3} + \frac{1}{2}n_{t_5}), \\ s_2 &= -1 + \frac{1}{n_2}(n_{r_1} - n_{r_4} - \frac{1}{2}n_{t_4}), \\ s_m &= 1 - \frac{1}{m}(n_{r_3} + n_{r_5} - n_{r_1} - n_{r_4} + \frac{1}{2}(n_{t_4} - n_{t_5})). \end{aligned} \quad (7)$$

From the condition that each dotted line must cross each dashed line once in a patch of size $p_1 N$ it then follows that in p_1 layers the average relative shift of the domain walls must be equal to N . The same arguments applied to the other cases then gives

$$N = p_1(s_m - s_2) = p_2(s_m - s_1) = q(s_1 - s_2). \quad (8)$$

Putting all these equations together, using the fact that the system size $N = n_1 + n_2 + m + 2(n_{r_2} - n_{r_5})$ one finds three independent relations among the tile densities. These can be rewritten as follows

$$\begin{aligned} n_{t_1}(n_{t_2} + n_{t_5}) &= 2(n_{t_4} + 2(n_{r_4} + n_{r_5}))(n_{r_1} + n_{r_2}) \\ &\quad + 2(n_{t_3} + 2(n_{r_3} + n_{r_2}))(n_{r_1} + n_{r_5}), \end{aligned} \quad (9)$$

$$\begin{aligned} n_{t_2}(n_{t_3} + 2(n_{r_4} + n_{r_5})) + 4n_{r_5}(n_{r_3} + n_{r_4}) &= \\ n_{t_5}(n_{t_4} + 2(n_{r_3} + n_{r_2})) + 4n_{r_2}(n_{r_3} + n_{r_4}), \end{aligned} \quad (10)$$

which are symmetric under the simultaneous exchange of indices $2 \leftrightarrow 5$ and $3 \leftrightarrow 4$, i.e. the mirror symmetry in the y -axis. Other relations may be obtained from (9) and (10) by applying a rotation over $2\pi/5$, i.e. shifting each index by one. Only three of them, however, are independent.

At the symmetric point each orientation occurs equally often, so we have $n_{t_i} = \frac{1}{5}n_{\text{tri}}$ and $n_{r_i} = \frac{1}{5}n_{\text{rect}}$, where n_{tri} and n_{rect} are the average total numbers of triangles and rectangles per layer. It follows then from (9) and the expression for the system size that at the symmetric point $n_{\text{tri}} = 10\tau^{-4}N$ and $n_{\text{rect}} = \frac{5}{2}\tau^{-5}N$. Using (4) we find that these values correspond with the following numbers of domain walls,

$$\tau n_2 = n_1 = m = \tau^{-2}N. \quad (11)$$

3. Bethe Ansatz

In this section we derive the Bethe Ansatz equations for the lattice model to diagonalise the transfer matrix. Again we make use of the fact that the triangles can be viewed as domain walls. Since these domain walls persist through the lattice we can think of them as being trajectories of three types of particles, where each number of particles is conserved. The transfer matrix \mathbf{T} , acting in the upwards direction, can be thought of as an evolution operator for these particles. Two types of the particles are then left movers whose trajectories are given by the solid and dashed lines. We call them of type 1 and type 2 respectively. The other type is a right mover and its trajectories are drawn as dotted lines. Because the number of particles of each type is conserved, \mathbf{T} is block diagonal in the particle numbers. In the sequel we shall diagonalise \mathbf{T} in each block separately by using a nested coordinate Bethe Ansatz [13].

A state α on a row of the lattice can be specified by the positions y_1, \dots, y_m of the right movers and by the positions x_1, \dots, x_n of the left movers with the specification that the lines i_1, \dots, i_{n_1} at positions $x_{i_1}, \dots, x_{i_{n_1}}$ are of type 1. Elements $\psi(\alpha)$ of an eigenvector of \mathbf{T} thus can be written explicitly as $\psi(i_1, \dots, i_{n_1} | x_1, \dots, x_n; y_1, \dots, y_m)$. The state which has no particles, i.e. the one with only the rectangles r_2 , is called the pseudo-vacuum. We make the following Ansatz for the form of the eigenvector,

$$\psi(i_1, \dots, i_{n_1} | x_1, \dots, x_n; y_1, \dots, y_m) = \sum_{\pi, \rho} \sum_{\mu} A(\Gamma) B(\mu) \prod_{a=1}^n z_{\pi_a}^{x_a} \prod_{b=1}^m w_{\rho_b}^{y_b} \prod_{c=1}^{n_1} \left[d^{x_{i_c}} \prod_{r=1}^{i_c-1} u(\mu_c, \pi_r) \right], \quad (12)$$

where the sum runs over all permutations $\mu = (\mu_1, \dots, \mu_{n_1})$ of the numbers $1, \dots, n_1$, all permutations π of the numbers $1, \dots, n$ and all permutations ρ of the numbers $1, \dots, m$. The coordinates x_a and y_b enter the Ansatz (12) as powers of complex numbers, z_i and w_j respectively, that are to be determined later. Factors in the eigenvector due to the order of the different types of right movers are given by the expression between brackets in (12). This is the so called nested part of the Ansatz which is a generalisation of the simple power for the coordinates. The index i_c may be seen as the ‘coordinate’ of right movers of type 1 relative to all right movers. This coordinate i_c determines the upper limit of a product over a complex valued function u which may still depend on the numbers z_i . The Ansatz (12) further contains an adjustable constant d whose presence will become clear below.

The amplitudes A depend on the permutations π and ρ and on the configuration of the left and right movers. These together are coded in a vector Γ in the following way. Let \mathbf{p} be the vector of coordinates x_i and y_j of all domain walls, ordered so that $p_j < p_{j+1}$. The entries of Γ are the elements of the permutations π and ρ . The order of succession in Γ of elements taken from π and ρ matches that of the elements of x and y respectively in \mathbf{p} . The amplitudes B only depend on the permutation μ .

If all the domain walls are separated the action of the transfer matrix is just a shift of each line to the right or to the left. The eigenvalue of \mathbf{T} corresponding to the vector (12) is therefore given by

$$\Lambda = r_2^{(N-n-m)/2} t_1^{2n-2n_1} t_2^{2m} (t_3^2 d)^{n_1} \prod_{a=1}^n z_a \prod_{b=1}^m w_b^{-1}, \quad (13)$$

where N is the size of the lattice. At places where different domain walls are close together, the action of \mathbf{T} is not given by a mere shift of all domain walls. Whenever there is a right mover just in front of a left mover and there are no other neighbouring walls, two things can happen. Either the right mover jumps over the left mover, which does not move, or the left mover jumps over the right mover, see figure 2. These

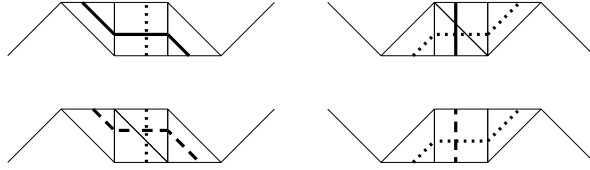


Figure 2. Two-particle collision diagrams. Upper line: Two types of collision of walls of type 1 and 3. Second line: Two types of collision of walls of type 2 and 3.

exceptions imply the following relations for (12) to be an eigenvector of \mathbf{T} .

$$\frac{A(\dots, \pi_k, \rho_l, \dots)}{A(\dots, \rho_l, \pi_k, \dots)} = \frac{r_3 d}{t_2^2} z_{\pi_k} w_{\rho_l} + \frac{r_1}{t_1^2} z_{\pi_k}^{-1} w_{\rho_l}^{-1}, \quad (14)$$

and they put the following constraints on the weights

$$r_3 d = t_4^2 \quad \text{and} \quad r_3 t_1^2 t_5^2 = r_1 t_3^2 t_4^2. \quad (15)$$

The reason for the constant d in the Ansatz (12) is now clear: if it were omitted there would be an additional constraint between the weights r_3 and t_4 . Scattering processes involving three particles of only two different types give the following restrictions on the amplitudes A ,

$$\frac{A(\dots, \pi_k, \pi_{k+1}, \dots)}{A(\dots, \pi_{k+1}, \pi_k, \dots)} = -\frac{z_{\pi_{k+1}}}{z_{\pi_k}}, \quad \frac{A(\dots, \rho_l, \rho_{l+1}, \dots)}{A(\dots, \rho_{l+1}, \rho_l, \dots)} = -\frac{w_{\rho_{l+1}}}{w_{\rho_l}}. \quad (16)$$

From these processes it also follows that the amplitudes B obey the equation

$$\sum_{\mu_p, \mu_{p+1}} B(\dots, \mu_p, \mu_{p+1}, \dots) z_{\pi_k} (u(\mu_{p+1}, \pi_k) - u(\mu_p, \pi_{k+1})) = 0. \quad (17)$$

By the sum in (17) we mean a sum over both permutations of the numbers μ_p and μ_{p+1} . A similar notation is used in the next two equations, which result from scattering

processes with three particles which are all of a different type.

$$\begin{aligned} & \sum_{\pi_k, \pi_{k+1}} A(\dots, \pi_k, \pi_{k+1}, \dots) z_{\pi_k} u(\mu_p, \pi_k) = \\ & \sum_{\pi_k, \pi_{k+1}} A(\dots, \pi_k, \pi_{k+1}, \dots) \left(\frac{r_2 r_3 r_5}{t_1^2 t_2^2 t_4^4} z_{\pi_k}^{-1} + \frac{t_1^2 r_4}{t_3^2 r_1} z_{\pi_k} z_{\pi_{k+1}}^2 \right). \end{aligned} \quad (18)$$

Equation (18) is satisfied (after A is eliminated using (16)), if u is of the form

$$u(\mu_p, \pi_k) = v_{\mu_p} + \frac{r_2 r_3 r_5}{t_1^2 t_2^2 t_4^4} z_{\pi_k}^{-2} - \frac{t_1^2 r_4}{t_3^2 r_1} z_{\pi_k}^2, \quad (19)$$

with any complex number v_{μ_p} . Substituting (19) into (17) it follows that the amplitudes B fulfil the relation

$$\frac{B(\dots, \mu_p, \mu_{p+1}, \dots)}{B(\dots, \mu_{p+1}, \mu_p, \dots)} = -1. \quad (20)$$

Using periodic boundary conditions, it follows from the form of the eigenvector (12) and the relations (14), (16) and (20) that the complex numbers z_i , w_j and v_k should obey the following Bethe Ansatz equations

$$w_j^{-N} = (-)^{m-1} \prod_{k=1}^m \left(\frac{w_j}{w_k} \right) \prod_{i=1}^n \left(\frac{t_4^2}{t_2^2} z_i w_j + \frac{r_1}{t_1^2} z_i^{-1} w_j^{-1} \right), \quad (21)$$

$$\begin{aligned} z_i^N &= (-)^{n-1} \prod_{k=1}^n \left(\frac{z_k}{z_i} \right) \prod_{j=1}^m \left(\frac{t_4^2}{t_2^2} z_i w_j + \frac{r_1}{t_1^2} z_i^{-1} w_j^{-1} \right) \times \\ & \prod_{l=1}^{n_1} \left(v_l + \frac{r_2 r_3 r_5}{t_1^2 t_2^2 t_4^4} z_i^{-2} - \frac{t_1^2 r_4}{t_3^2 r_1} z_i^2 \right), \end{aligned} \quad (22)$$

$$(-)^{n_1-1} = \left(\frac{t_4^2}{r_3} \right)^N \prod_{i=1}^n \left(v_l + \frac{r_2 r_3 r_5}{t_1^2 t_2^2 t_4^4} z_i^{-2} - \frac{t_1^2 r_4}{t_3^2 r_1} z_i^2 \right). \quad (23)$$

To rewrite the BA equations in a more suitable form we introduce the following variables,

$$\begin{aligned} \tilde{\xi}_i &= \left(\frac{r_4 t_1^4 t_4^4}{r_1 r_2 r_3 r_5} \right)^{1/2} z_i^2, \quad \psi_j = - \left(\frac{r_1 r_4 t_2^4}{r_2 r_3 r_5} \right)^{1/2} w_j^{-2}, \\ u_l - u_l^{-1} &= \left(\frac{r_1 t_3^4 t_4^4}{r_2 r_3 r_4 r_5} \right)^{1/2} v_l. \end{aligned} \quad (24)$$

The BA equations then become

$$(-\psi_j)^{(N+n+m)/2} = (-)^{m-1} C \prod_{i=1}^n \tilde{\xi}_i^{-1/2} \prod_{k=1}^m (-\psi_k)^{1/2} \prod_{i=1}^n (\tilde{\xi}_i - \psi_j), \quad (25)$$

$$\begin{aligned} \tilde{\xi}_i^{(N+n+m)/2} &= (-)^{n-1} D \prod_{k=1}^n \tilde{\xi}_k^{1/2} \prod_{j=1}^m (-\psi_j)^{-1/2} \prod_{l=1}^{n_1} u_l^{-1} \times \\ & \prod_{j=1}^m (\tilde{\xi}_i - \psi_j) \prod_{l=1}^{n_1} (u_l - \tilde{\xi}_i)(u_l + \tilde{\xi}_i^{-1}), \end{aligned} \quad (26)$$

$$u_l^n = (-)^{n_1-1} E \prod_{i=1}^n (u_l - \tilde{\xi}_i)(u_l + \tilde{\xi}_i^{-1}), \quad (27)$$

where C, D and E are given by

$$\begin{aligned} C &= \left(\frac{r_1 r_4 t_2^4}{r_2 r_3 r_5} \right)^{N/4} \left(\frac{r_1 t_4^2}{t_1^2 t_2^2} \right)^{n/2} \\ D &= \left(\frac{r_4 t_1^4 t_4^4}{r_1 r_2 r_3 r_5} \right)^{N/4} \left(\frac{r_1 t_4^2}{t_1^2 t_2^2} \right)^{m/2} \left(\frac{r_2 r_3 r_4 r_5}{r_1 t_3^4 t_4^4} \right)^{n_1/2} \\ E &= \left(\frac{t_4^2}{r_3} \right)^N \left(\frac{r_2 r_3 r_4 r_5}{r_1 t_3^4 t_4^4} \right)^{n/2}. \end{aligned} \quad (28)$$

The eigenvalue in terms of these new variables is then given by

$$\Lambda = r_2^{N/2} \left(\frac{r_1 r_3 r_5 t_1^4}{r_2 r_4 t_4^4} \right)^{n/4} \left(\frac{r_3 r_5 t_2^4}{r_1 r_2 r_4} \right)^{m/4} \left(\frac{t_3^2 t_4^2}{r_3 t_1^2} \right)^{n_1} \prod_{i=1}^n \tilde{\xi}_i^{1/2} \prod_{j=1}^m (-\psi_j)^{1/2}. \quad (29)$$

In summary we have shown in this section that the Bethe Ansatz equations (25), (26) and (27) with the definitions (28) diagonalise the transfer matrix \mathbf{T} for arbitrary choice of the weights except for the one constraint $r_3 t_1^2 t_5^2 = r_1 t_3^2 t_4^2$. It thus follows that the point of maximum symmetry, where $r_i = r$ for $i \neq 2$ † and $t_i = t$, is included in the spectrum obtained by this Ansatz. The eigenvalue of \mathbf{T} in terms of solutions of the Bethe Ansatz equations is given by (29).

4. Integral equations

To calculate the entropy, we put $t_i = 1$, $r_2 = e^{\mu_1}$ and $r_1 = r_3 = r_4 = r_5 = e^{\mu_2}$. The chemical potentials μ_1 and μ_2 have to be adjusted such that all configurations in the original undeformed tiling model are weighted properly. The difference between μ_1 and μ_2 compensates for the fact that the area of the transformed tile r_2 is twice that of the other transformed rectangles. If we want to weight the original rectangles in the random tiling equally it follows that they must satisfy [11]

$$\mu_1 - \mu_2 = N^{-1} \log \Lambda_{\max}. \quad (30)$$

One finds numerically that the maximum of the entropy of the tiling model is at the point of maximum symmetry, i.e. where all configurations are weighted equally, in agreement with the first random tiling hypothesis [14]. According to (11) this is in the sector $n_1 = m = \tau^{-2}N$, $n_2 = \tau^{-3}N$, corresponding to tile fractions $n_{\text{rect}} = \frac{5}{2}\tau^{-5}N$ and $n_{\text{tri}} = 10\tau^{-4}N$.

It is also observed numerically that each of the roots u_l approximates one of the roots $\tilde{\xi}_i$ in exponentially good precision, see figure 3. For reasons that will become clear

† We need to tune r_2 to compensate for the change in area induced by the transformation to the lattice.

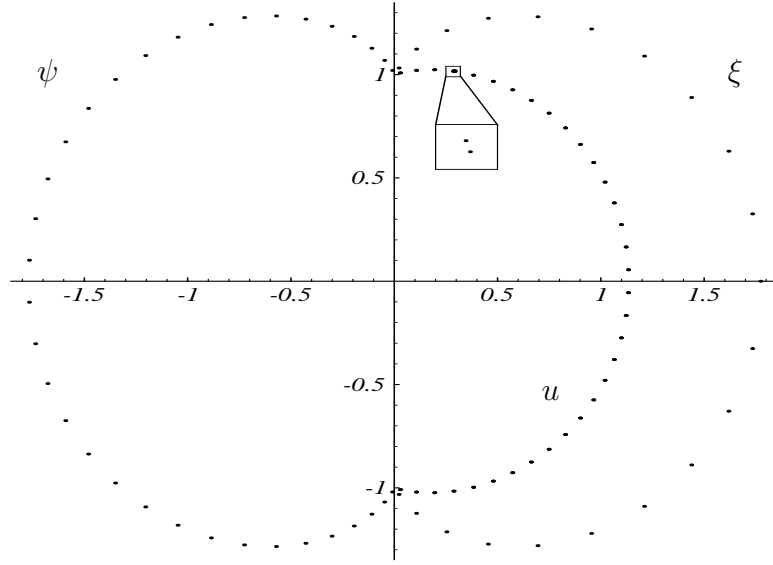


Figure 3. Distribution of roots for the largest eigenvalue ($N = 89$, $n_1 = m = 34$, $n_2 = 21$). The left curve corresponds to the roots ψ_i and the outer right curve corresponds to some subset $\{\xi_i\}$ of the roots $\tilde{\xi}_i$. The inner right curve actually consists of two curves corresponding to the roots u_i and the subset of the roots $\tilde{\xi}_i$ complementary to $\{\xi_i\}$. Note that the inset is not on scale.

below, we define the roots ξ_i now as the subset of the roots $\tilde{\xi}_i$ *not* approximated by one of the u_l and we introduce the following notation

$$s_\xi = \prod_{i=1}^{n_2} \xi_i^{1/2}, \quad s_\psi = \prod_{j=1}^m (-\psi_j)^{1/2}, \quad s_u = \prod_{l=1}^{n_1} u_l^{1/2}. \quad (31)$$

By writing $\tilde{\xi} = u_l + \varepsilon_l$ for those roots $\tilde{\xi}$ that are approximated by one of the u_l and using the above abbreviations, equation (26) splits up in the following two sets of equations,

$$\begin{aligned} \xi_i^{(N+3n_1+n_2+m)/2} &= (-)^{n_2-1} D s_\xi s_u s_\psi^{-1} \prod_{j=1}^m (\xi_i - \psi_j) \prod_{l=1}^{n_1} (\xi_i - u_l) (\xi_i + u_l^{-1}), \\ (u_k + \varepsilon_k)^{(N+n_1+n_2+m)/2} &= (-)^{n_1+n_2-1} D s_\xi s_u s_\psi^{-1} \prod_{j=1}^m (u_k - \psi_j + \varepsilon_k) \times \\ &\quad \prod_{l=1}^{n_1} (u_l - u_k - \varepsilon_k) \left(1 + u_l^{-1} (u_k + \varepsilon_k)^{-1}\right). \end{aligned} \quad (32)$$

Similarly, substituting $\tilde{\xi} = u + \varepsilon$ in (27) results in

$$\begin{aligned} (-)^{n_1-1} E^{-1} u_l^{n_2} &= \prod_{k=1}^{n_1} (u_l - u_k - \varepsilon_k) \left(1 + u_l^{-1} (u_k + \varepsilon_k)^{-1}\right) \times \\ &\quad \prod_{i=1}^{n_2} (u_l - \xi_i) (u_l + \xi_i^{-1}). \end{aligned} \quad (34)$$

In the thermodynamic limit all ε_k vanish exponentially in N . Equation (34) can then be used to remove the product over the variables u in (33) and we arrive at the following equation which approximates the original BA equation (33),

$$u_k^{(N+n_1-n_2+m)/2} = (-)^{n_1-1} D E^{-1} s_\xi s_u s_\psi^{-1} \prod_{j=1}^m (u_k - \psi_j) \times \prod_{i=1}^{n_2} (\xi_i - u_k)^{-1} (u_k + \xi_i^{-1})^{-1} + \mathcal{O}(e^{-N}), \quad (35)$$

Consider now the BA equation (25) as a function of ψ_j . Taking the logarithm on both sides of (25) we define the function F_ψ by

$$F_\psi(z) = \log(-z) - \frac{2}{N + n_1 + n_2 + m} \left[\sum_{i=1}^{n_2} \log(\xi_i - z) + \sum_{l=1}^{n_1} \log(u_l - z) - \frac{1}{4} N \mu_1 + \frac{1}{2} (n_1 + n_2) \mu_2 - \log \frac{s_\xi s_u}{s_\psi} \right], \quad (36)$$

so that $\Re F_\psi(\psi_j) = 0$. Similar functions $F_\xi(z)$ and $F_u(z)$ are defined by taking the logarithm of equations (32) and (35) respectively. The BA equations (25), (32) and (35) are then equivalent to

$$\begin{aligned} \frac{1}{2} (N + n_1 + n_2 + m) F_\psi(\psi_k) &= 2\pi i I_k, \\ \frac{1}{2} (N + 3n_1 + n_2 + m) F_\xi(\xi_k) &= 2\pi i J_k, \\ \frac{1}{2} (N + n_1 - n_2 + m) F_u(u_k) &= 2\pi i K_k, \end{aligned} \quad (37)$$

where I_k , J_k and K_k are either integers or half-integers. From numerical calculations it follows that the numbers I_k , J_k and K_k for the solutions of the BA equations for the largest eigenvalue are consecutive, more precisely

$$\begin{aligned} I_k &= \frac{1}{2} (m + 1 - 2k), \quad (k = 1, \dots, m) \\ J_k &= \frac{1}{2} (n_2 + 1 - 2k), \quad (k = 1, \dots, n_2) \\ K_k &= \frac{1}{2} (n_1 + 1 - 2k), \quad (k = 1, \dots, n_1) \end{aligned} \quad (38)$$

We will assume that (38) holds in the thermodynamic limit. It is for this reason that we introduced the variables ξ instead of $\tilde{\xi}$. The function analogous to (36) defined from (26) does not take consecutive multiples of $2\pi i$ when evaluated at the roots $\tilde{\xi}_k$. It is clear from (38) that the derivatives f of the functions F are up to a factor precisely the densities of the Bethe Ansatz roots. They allow us to transform the sums in the logarithmic form of the BA equations into integrals. For brevity we define

$$\alpha = \frac{1 + 3Q_1 + Q_2 + Q_m}{1 + Q}, \quad \beta = \frac{1 + Q_1 - Q_2 + Q_m}{1 + Q}, \quad (39)$$

where $Q = Q_1 + Q_2 + Q_m$. Taking into account the root distribution (38) we thus arrive at the following integral equations for the functions f ,

$$f_\psi(z) = \frac{1}{z} + \frac{\alpha}{2\pi i} \int_{\xi_1}^{\xi_{n_2}} \frac{f_\xi(\xi)}{z - \xi} d\xi + \frac{\beta}{2\pi i} \int_{u_1}^{u_{n_1}} \frac{f_u(u)}{z - u} du, \quad (40)$$

$$f_\xi(z) = \frac{1}{z} + \frac{\beta}{2\pi i \alpha} \left[\int_{u_1}^{u_{n_1}} \frac{f_u(u)}{z - u} du + \int_{-u_1^{-1}}^{-u_{n_1}^{-1}} \frac{u^{-2} f_u(-u^{-1})}{z - u} du \right] + \frac{1}{2\pi i \alpha} \int_{\psi_1}^{\psi_m} \frac{f_\psi(\psi)}{z - \psi} d\psi, \quad (41)$$

$$f_u(z) = \frac{1}{z} - \frac{\alpha}{2\pi i \beta} \left[\int_{\xi_1}^{\xi_{n_2}} \frac{f_\xi(\xi)}{z - \xi} d\xi + \int_{-\xi_1^{-1}}^{-\xi_{n_2}^{-1}} \frac{\xi^{-2} f_\xi(-\xi^{-1})}{z - \xi} d\xi \right] + \frac{1}{2\pi i \beta} \int_{\psi_1}^{\psi_m} \frac{f_\psi(\psi)}{z - \psi} d\psi, \quad (42)$$

where the integrals are taken along the locus of the roots ξ , ψ and u and $-\xi^{-1}$, $-\psi^{-1}$ and $-u^{-1}$. These integration contours in the complex plane are schematically shown in figure 4.

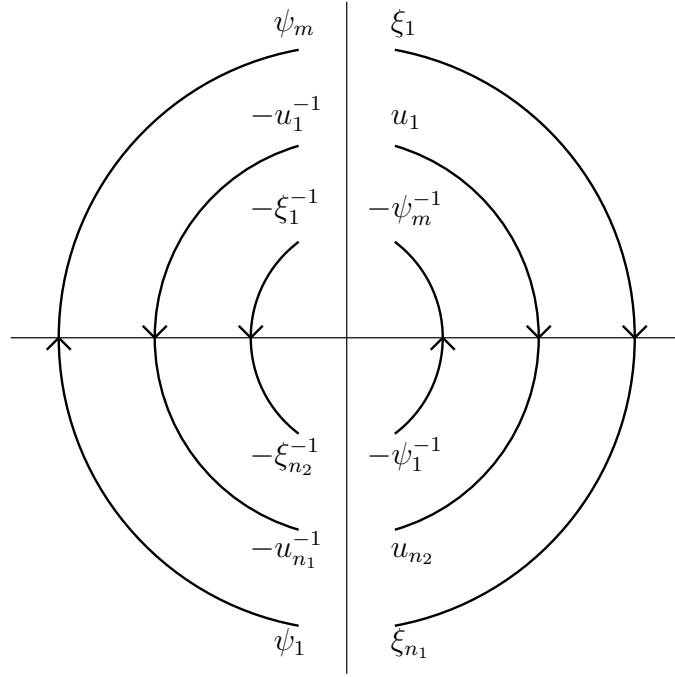


Figure 4. Schematic picture of the solution curves of the BA equations.

5. Monodromy properties

From the integral equations it is immediately seen that the integration contours are cuts in the complex plane of the functions $f_\xi(z)$, $f_\psi(z)$, $f_u(z)$, $z^{-2}f_\xi(-z^{-1})$,

$z^{-2}f_\psi(-z^{-1})$ and $z^{-2}f_u(-z^{-1})$. Each of these functions has jumps across some of the cuts whose magnitudes are given by linear combinations of the above six functions. The analytic continuation across the cuts of these functions is now determined by compensating for the jump and can be written in terms of monodromy operators, one for each cut. The analytic continuations across the different cuts of a function $G(z) = \sum_{i=\xi,\psi,u}(a_i f_i(z) + b_i z^{-2} f_i(-z^{-1}))$ are given by the following matrices which act on the vector $\mathbf{a} = (a_\xi, a_\psi, a_u, b_\xi, b_\psi, b_u)$,

$$\begin{aligned}
\Gamma_\psi &= I - \alpha^{-1}E_{21} - \beta^{-1}E_{23}, \\
\Gamma_{\psi^{-1}} &= I - \alpha^{-1}E_{54} - \beta^{-1}E_{56}, \\
\Gamma_\xi &= I + \alpha E_{12} - \alpha\beta^{-1}(E_{13} + E_{16}), \\
\Gamma_{\xi^{-1}} &= I + \alpha E_{45} - \alpha\beta^{-1}(E_{43} + E_{46}), \\
\Gamma_u &= I + \beta E_{32} + \beta\alpha^{-1}(E_{31} + E_{34}), \\
\Gamma_{u^{-1}} &= I + \beta E_{65} + \beta\alpha^{-1}(E_{61} + E_{64}),
\end{aligned} \tag{43}$$

where I is the 6×6 unit matrix and E_{ij} is the matrix with a 1 at the entry ij and 0's everywhere else. As a result, several linear combinations of the six functions, following from these monodromy operations, correspond to different sheets of the Riemann surface of one function.

The continuation of a function $G(z)$ starting at and returning to the origin across all of the six curves is given by the monodromy operator $\Gamma = \Gamma_{\xi^{-1}}\Gamma_{u^{-1}}\Gamma_\psi\Gamma_\xi\Gamma_u\Gamma_{\psi^{-1}}$ which has the property that $\Gamma^5 = 1$. This means that if the curves in figure 4 have the same endpoints, say b for the common endpoint in the upper half plane and b^* for that in the lower half plane, that function is single valued in terms of the variable s :

$$s(z) = \left(\frac{zb^{-1} - 1}{1 - zb^{*-1}} \right)^{1/5}, \quad z(s) = b \frac{1 + s^5}{1 + bb^{*-1}s^5}. \tag{44}$$

When the BA-curves have the same endpoints, Γ is the only non trivial monodromy operator and the Riemann surface of $G(z)$ breaks up into infinitely many disconnected parts each with only five sheets. These are all mapped onto the plane by (44), from which it is easily seen that, apart from the branch points $z = b$ and $z = b^*$, each point in the z -plane has five images on the s -plane. As can be seen from figure 3, for the largest eigenvalue the curves do indeed have the same endpoints, in particular they meet at $b = -b^* = i$. The situation is rather similar to what happens in the square triangle [5] and the octagonal rectangle triangle tiling [6], where also the BA curves close, but there the monodromy is of order 6 and 4 respectively. Although we do not understand the deeper reason for this, it will become obvious in the sequel that the order of the monodromy must relate to the symmetry of the tiling to produce the right quadratic irrationalities.

In the following we show that the closing of the curves enables us to calculate the largest eigenvalue explicitly. Note that the six curves can only have the same endpoints if $b = -b^{-1} = i$, see figure 4, in contrast to the square triangle and the octagonal rectangle triangle tiling, where the common endpoints need not lie on the imaginary axis. We will, however, use the notation $b = |b|e^{i\gamma}$ for the common endpoint of the curves, for it may turn out in the future that for infinitesimal values of γ still something can be said.

Aside from the cuts, the form Gdz has only simple poles at $z = 0$ and at $z = \infty$. The poles and their residues of the single valued function are thus given by the poles and residues on each of the sheets. The functional form of $G(z)$ on other parts of the sheet and on the other sheets is directly determined by the monodromy operators (43). In particular, the value of the residues can then be read off from the integral equations (40), (41) and (42). We choose $G(z)$ to be equal to $f_\psi(z)$ near $z = 0$ on the sheet with $s_1 = e^{i\pi/5}$. Its form near $z = 0$ on the sheets with $s_{2k-1} = e^{(2k-1)i\pi/5}$ is obtained by applying Γ^k . The functional forms of the function $G(z)$ near $z = \infty$ on the sheets with $s_{2k} = e^{2i(k\pi-\gamma)/5}$ are obtained by analytic continuation, i.e. by applying $\Gamma_\xi\Gamma_u\Gamma_{\psi^{-1}}$ on each of the functions corresponding to s_{2k-1} . The poles s_n and residues R_n thus obtained of this function G are shown in table 1.

Table 1. Poles and residues of the form $G(z)dz$. The two columns on the left list the poles of $G(z)dz$ on the z - and on the s -plane respectively. The third column gives the functional form of $G(z)$ near those poles and the fourth column the value of the residues of these poles.

z	s_n	G	$R_n = \text{Res}_{-1}(Gdz)$
0	$e^{\pi i/5}$	$f_\psi(z)$	1
∞	$e^{2i(\pi-\gamma)/5}$	$f_\psi(z) + \beta f_u(z)$	$\frac{-2(1+Q_2)}{1+Q}$
0	$-e^{-2\pi i/5}$	$\beta f_u(z) - \alpha z^{-2} f_\xi(-z^{-1})$	$\frac{2}{1+Q}$
∞	$-e^{-i(\pi+2\gamma)/5}$	$-\alpha z^{-2} f_\xi(-z^{-1}) + z^{-2} f_\psi(-z^{-1})$	$\frac{-2Q_1}{1+Q}$
0	-1	$z^{-2} f_\psi(-z^{-1})$	$-\frac{1+Q_m-Q_1-Q_2}{1+Q}$
∞	$-e^{i(\pi-2\gamma)/5}$	$z^{-2} f_\psi(-z^{-1})$	1
0	$-e^{2i\pi/5}$	$z^{-2} f_\psi(-z^{-1}) + \beta z^{-2} f_u(-z^{-1})$	$\frac{-2(1+Q_2)}{1+Q}$
∞	$e^{-2i(\pi+\gamma)/5}$	$\beta z^{-2} f_u(-z^{-1}) - \alpha f_\xi(z)$	$\frac{2}{1+Q}$
0	$e^{-i\pi/5}$	$-\alpha f_\xi(z) + f_\psi(z)$	$\frac{-2Q_1}{1+Q}$
∞	$e^{-2i\gamma/5}$	$f_\psi(z)$	$-\frac{1+Q_m-Q_1-Q_2}{1+Q}$

The form Gdz is now uniquely determined by its poles and residues,

$$Gdz = \sum_{n=1}^{10} \frac{R_n}{s - s_n} ds. \quad (45)$$

Recall that we are working with approximated BA equations which are valid for the largest eigenvalue, for which $Q_1 = Q_m = \tau^{-2}$, $Q_2 = \tau^{-3}$ and thus $Q = 1$. We do not know at the moment if the approximation is valid for other sectors as well. The closing of the three curves at $b = i$ ($\gamma = 0$), however, is a fact that only holds for the largest eigenvalue. The above arguments for calculating Gdz therefore are valid for this sector only, for which Gdz is given by

$$Gdz = (se^{-2i\pi/5} + s^{-1}e^{2i\pi/5})\tau^{-1} \frac{dz}{z}. \quad (46)$$

6. Solution of definite integrals

In this section we calculate some definite integrals of the form (46), resulting in an exact expression for the maximum of the entropy. To remove singularities in the expressions to follow, we introduce the following forms

$$g_n dz = \frac{R_{2n-1}}{s - s_{2n-1}} ds. \quad (47)$$

In the z -plane we can calculate the following integrals using the fact that $b = i$ is a solution of the BA equations and that we have a precise control of the singularity at $z = 0$ by using the mapping (44) to the s -plane.

$$\begin{aligned} J_{1,0} &= \Re \left[\int_b^0 (f_\psi(z) - g_1) dz \right] = \Re \lim_{s \rightarrow e^{i\pi/5}} \left[F_\psi(z(s)) - \log(s - e^{i\pi/5}) \right] \\ &= \log(5/2) - N^{-1} \log \Lambda + \mu_1 \frac{1}{2} - \mu_2 \tau^{-2}, \end{aligned} \quad (48)$$

$$\begin{aligned} J_{2,0} &= \Re \left[\int_b^0 (\beta f_u(z) - \alpha z^{-2} f_\xi(-z^{-1}) - g_2) dz \right] \\ &= \log(5/2) - 2N^{-1} \log s_\psi + \mu_1 \frac{1}{2} \tau^{-1} - \mu_2 \tau^{-2}, \end{aligned} \quad (49)$$

$$\begin{aligned} J_{3,0} &= \Re \left[\int_b^0 (z^{-2} f_\psi(-z^{-1}) - g_3) dz \right] \\ &= -\tau^{-2} \log(5/2) + N^{-1} \log \Lambda - 2N^{-1} \log s_\psi - \mu_2 \tau^{-3}, \end{aligned} \quad (50)$$

$$\begin{aligned} J_{4,0} &= \Re \left[\int_b^0 (z^{-2} f_\psi(-z^{-1}) + \beta z^{-2} f_u(-z^{-1}) - g_4) dz \right] \\ &= -2\tau^{-1} \log(5/2) + \mu_1 \tau^{-1} - \mu_2 2\tau^{-2}, \end{aligned} \quad (51)$$

$$\begin{aligned} J_{5,0} &= \Re \left[\int_b^0 (-\alpha f_\xi(z) + f_\psi(z)) - g_5) dz \right] \\ &= -\tau^{-2} \log(5/2) + \mu_1 \frac{1}{2} \tau^{-2} - \mu_2 \tau^{-3} = \frac{1}{2\tau} J_{4,0}. \end{aligned} \quad (52)$$

The same integrals on the s -plane restricted to the symmetric point are, using (45),

$$\begin{aligned}
J_{1,0} &= \sum_{n=2}^{10} R_n \log |e^{i\pi/5} - s_n| = \tau \log \tau - \log \sin(2\pi/5), \\
J_{2,0} &= \tau \log \tau - \log \sin(2\pi/5), \\
J_{3,0} &= -\tau^{-1} \log \tau + \tau^{-2} \log \sin(2\pi/5), \\
J_{4,0} &= -2 \log \tau + 2\tau^{-1} \log \sin(2\pi/5), \\
J_{5,0} &= -\tau^{-1} \log \tau + \tau^{-2} \log \sin(2\pi/5).
\end{aligned} \tag{53}$$

Equating both sets of integrals gives the following solution

$$\begin{aligned}
4\tau^{-1}s_\psi &= \mu_1 - (1 + \tau^{-3})\mu_2 = N^{-1} \log \Lambda - \tau^{-3}\mu_2 \\
&= \frac{1}{2} \left(\log \frac{5^5}{4^4} - 2\sqrt{5} \log \tau \right).
\end{aligned} \tag{54}$$

Note that this solution precisely corresponds to the maximum of the entropy for the original tiling model according to (30). The total number of rectangles per site, $Q_{\text{rect}} = n_{\text{rect}}/N$, on the symmetric point is $\frac{5}{2}\tau^{-5}$, so that the entropy per site is given by

$$\sigma_N = N^{-1} \log \Lambda - \frac{1}{2}\tau^{-5}(\mu_1 + 4\mu_2) = \frac{5}{2}\tau^{-2}(N^{-1} \log \Lambda - \tau^{-3}\mu_2). \tag{55}$$

The number of vertices per site n_v is given by

$$n_v = \frac{1}{2}Q_{\text{tri}} + Q_{\text{rect}} = \frac{5}{2}\tau^{-4}(2 + \tau^{-1}) = \frac{5}{2}\tau^{-2}. \tag{56}$$

Thus, the entropy per vertex σ_v is finally given by

$$\sigma_v = N^{-1} \log \Lambda - \tau^{-3}\mu_2 = \frac{1}{2} \left(\log \frac{5^5}{4^4} - 2\sqrt{5} \log \tau \right). \tag{57}$$

7. Conclusion

In this paper we showed that a decagonal random tiling model of rectangles and triangles is solvable using the Bethe Ansatz technique. We derived the Bethe Ansatz equations that diagonalise the transfer matrix for this model. These equations contain all information about the model and they in principle present a huge reduction of computational problems concerning the system size. For this tiling model however, some of the roots of the BA equations almost coincide, which makes it difficult to extract high precision data. On the other hand, it enabled us to write down approximate BA equations which are exact at the symmetric point in the thermodynamic limit. Using these equations we were able to find an exact expression for the maximum of the entropy. The validity of the approximation outside the symmetric point still has to be further investigated. We hope to be able to find analytic expressions for the phason

elastic constants as well, although in contrast to the solutions of the dodecagonal square-triangle [4, 5] and the octagonal rectangle triangle [6, 7] it is not apparent if our solution can be extended off the symmetric point. Recently, Kalugin [15] showed for the square triangle model that also critical exponents may be calculated exactly from the BA equations.

Acknowledgments

We thank M Martins for discussions and A Verberkmoes for a reading of the manuscript. This research was supported by ‘Stichting Fundamenteel Onderzoek der Materie’ which is financially supported by the Dutch foundation for scientific research NWO.

References

- [1] Coddens G 1997 Models for assisted phason hopping and phason elasticity in icosahedral quasicrystals *Int. J. Mod. Phys. B* **11** 1679.
- [2] Joseph D, Ritsch S and Beeli C 1997 Distinguishing quasiperiodic from random order in high-resolution TEM images *Phys. Rev. B* **55** 8175.
- [3] Joseph D and Elser V 1997 A model of quasicrystal growth *Phys. Rev. Lett.* **79** 1066.
- [4] Widom M 1993 Bethe Ansatz solution of the square-triangle random tiling model *Phys. Rev. Lett.* **70** 2094.
- [5] Kalugin P 1994 The square-triangle random-tiling model in the thermodynamic limit *J. Phys. A: Math. Gen.* **27** 3599.
- [6] Gier J de and Nienhuis B 1996 Exact solution of an octagonal random tiling *Phys. Rev. Lett.* **76** 2918.
- [7] Gier J de and Nienhuis B 1997 The exact solution of an octagonal rectangle-triangle random tiling *J. Stat. Phys.* **87** 415.
- [8] Cockayne E 1995 Dense quasiperiodic decagonal disc packing *Phys. Rev. B* **51** 14958.
- [9] Oxborrow M and Mihalkovič M 1995 Lurking in the wings: A random-tiling geometry for decagonal AlPdMn *Aperiodic '94* eds Chapuis G and Paciorek W (Singapore: World Scientific) 178.
- [10] Roth J and Henley C L 1997 A new binary decagonal Frank-Kasper quasicrystal phase *Phil. Mag. A* **75** 861.
- [11] Li W, Park H and Widom M 1992 Phase diagram of a random tiling quasicrystal *J. Stat. Phys.* **66** 1.
- [12] Henley C L 1988 Random tilings with quasicrystal order *J. Phys. A: Math. Gen.* **21** 1649.
- [13] Baxter R 1970 Colorings of a hexagonal lattice *J. Math. Phys.* **11** 784.
- [14] Henley C L 1991 Random tiling models *Quasicrystals: The State of the Art* eds Steinhardt P J and DiVincenzo D P (Singapore: World Scientific) 429.
- [15] Kalugin P A 1997 Low-lying excitations in the square-triangle random tiling model *J. Phys. A: Math. Gen.* **30** 7077.